can be produced on a five-membered ring containing a sulfur atom. The species previously observed in solution by Grossi et al.[12] corresponds to **7**, where A is a methyl group. The experimental coupling constants A_{iso}(H4) = 14.7 G and A_{is3}(N) = 3.9 G are in good accordance with the values calculated for **7** from the Fermi contact interaction (A_{iso}(H4) = 13.3 G, A_{iso}(N) = 5.0 G).

In accordance with the ab initio results obtained for the allyl and azaallyl radicals, the experimental hyperfine couplings[13] obtained for radical **9** clearly show a similar isotropic coupling

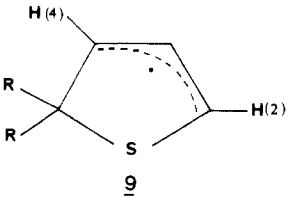

9

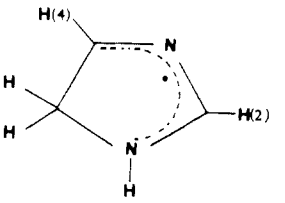

10

constant for protons H(2) and H(4). These results are in contrast with those previously reported[37,39] for the radical **10** resulting from hydrogen addition on an imidazole ring; for this latter radical the two couplings for protons H(2) and H(4) were different and the unpaired electron appeared to be delocalized onto two carbon and two nitrogen atoms.

Most of the observed heteroatoms containing allylic radicals correspond to cationic species which have been produced by ring opening of saturated small heterocycles; for example, $(CH_2–NH–CH_2)^{\bullet+}$ [7,8] and $(CH_2–O–CH_2)^{\bullet+}$ [40-42] have recently been formed by irradiation of aziridine and oxirane, respectively. These cations exhibit a ^{1}H isotropic coupling with the protons in the exo position, which is slightly higher than that found for RCH=N̊=CBrR ($CH_2–NH–CH_2^{\bullet+}$: 17 G;[7] $CH_2–O–CH_2^{\bullet+}$: 16.4 G;[40] RHC–N–CBrR$^{\bullet}$: 12.6 G), but the major difference resides in the bent structure which is more pronounced for the neutral radical (optimized structures: $CH_2–N–CH_2^{\bullet}$: 119°; $CH_2–NH–CH_2^{\bullet+}$: 127°;[9] $CH_2–O–CH_2^{\bullet+}$: 131° [3]). Unfortunately, neither the theoretical coupling tensors nor the orientations of the experimental hyperfine eigenvectors are available for these allylic cations, and further comparison would be premature.

Radiation Process

The reaction mechanism giving rise to the formation of RHC=N̊=CBrR is similar to previous observations in the thiophene series:[13] at low temperature, radical pairs are formed; they are not stable with increasing temperature and near 300 K the spectrum of an allyl-type radical is observed. This species results from the addition of a radical R on a carbon adjacent to the sulfur atom; the R fragment is, however, located too far from the allylic moiety to be identified.

Acknowledgment. We are indebted to Professor Gamba for a copy of his spin annihilation procedure within the GAUSSIAN 80 program. We thank Professor L. D. Kispert for preliminary ENDOR measurement. The financial support of the Swiss National Science Foundation is gratefully acknowledged.

Supplementary Material Available: Tables of bond lengths and angles and anisotropic displacement parameters along with a computer-generated plot, tables of form factors, and experimental and simulated ESR spectra corresponding to intermediate orientations of the magnetic field (25 pages). Ordering information is given on any current masthead page.

(37) Lamotte, B. Ph.D. Thesis, 1968, Universit de Grenoble.
(38) Westhof, E.; Flossmann, W. *J. Am. Chem. Soc.* **1975**, *97*, 6622.
(39) Kasai, P. H.; McLeod, D., Jr. *J. Am. Chem. Soc.* **1973**, *95*, 27.
(40) Snow, L. D.; Wang, J. T.; Williams, F. *Chem. Phys. Lett.* **1983**, *100*, 193.
(41) Symons, M. C. R.; Wren, B. W. *Tetrahedron Lett.* **1983**, 2315.
(42) Bally, T.; Nitsche, S.; Haselbach, E. *Helv. Chim. Acta* **1984**, *67*, 86.

A Time-Resolved ESR Study of the Kinetics of Spin Trapping by Nitromethane *aci*-Anion[1]

Keith P. Madden,* Hitoshi Taniguchi, and Richard W. Fessenden

Contribution from the Radiation Laboratory and Department of Chemistry, University of Notre Dame, Notre Dame, Indiana 46556-0768. *Received August 21, 1987*

Abstract: The kinetics of spin trapping by the *aci*-anion of nitromethane have been studied for some representative radicals in aqueous solution by using time-resolved ESR with in situ radiolysis. In nearly all cases, reaction of a radical R produced an adduct $RCH_2NO_2^-$. However, these time-resolved experiments showed that $^{\bullet}CH_2O^-$ produces both an adduct and the radical anion of nitromethane. Second-order rate constants varied from 1.4×10^7 M^{-1} s^{-1} for CO_2^- to 3.8×10^8 for the *p*-carboxyphenyl radical. Reducing radicals (CO_2^-, CH_2O^-, $(CH_3)_2COH$, and $(CH_3)_2CO^-$) react less rapidly than alkyl radicals ($CH_2CO_2^-$, CH_3) which in turn react less rapidly than σ radicals (*p*-carboxyphenyl and $CONH_2$).

Spin trapping[2,3] has greatly extended the use of electron spin resonance as a qualitative tool in the study of free-radical reactions by augmenting its intrinsic sensitivity and selectivity. In this way, ESR is provided with the ability to visualize radicals that are otherwise unobservable due to short radical lifetimes, complex hyperfine structure, or unfavorable magnetic relaxation rates. Quantitative spin trapping, dubbed "spin counting" by Janzen,[4] relies on the correlation of spin adduct ESR intensity with the initial concentration of the trapped transient radical species. The spin adduct intensity in a conventional steady-state ESR experiment (SSESR) is a reflection of spin-adduct steady-state concentration, determined by the rates of adduct formation and

(1) The research described herein was supported by the Office of Basic Energy Sciences of the Department of Energy. This is Document No. NDRL-3024 from the Notre Dame Radiation Laboratory.
(2) (a) Lagercrantz, C. *J. Phys. Chem.* **1971**, *75*, 3466-75. (b) Janzen, E. G. *Acc. Chem. Res.* **1971**, *4*, 31-40.
(3) (a) Perkins, M. J. "Spin Trapping" In *Advances in Physical Organic Chemistry*; Gold, V., Bethell, D., Eds.; Academic Press: New York, 1980; Vol. 17, pp 1-64. (b) Janzen, E. G. "A Critical Review of Spin Trapping in Biological Systems" In *Free Radicals in Biology*; Pryor, W. A., Ed.; Academic Press: New York, 1980; Vol. IV, pp 115-54.
(4) Janzen, E. G.; Evans, C. A.; Nishi, Y. *J. Am. Chem. Soc.* **1972**, *94*, 8236-8.

0002-7863/88/1510-2753$01.50/0

decay.[5] The rates of adduct formation have been determined for a few cases in competition experiments, timing the spin trapping rate against a "radical clock"[6] such as decarboxylation of benzoyloxy radicals,[4] abstraction of hydrogen atoms by *tert*-butoxy radicals,[7,8] alkoxy to hydroxyalkyl radical interconversion,[9,10] acyl radical fragmentation,[11,12] phenyl addition to benzene,[13] hydrogen abstraction by phenyl radicals[14] or CF_3,[15] or irreversible radical cyclization.[16,17] Even fewer studies have been performed to investigate spin adduct decay.[8,18] All of these studies have been indirect, with use of the "radical clock" concept upon a static system to infer the kinetics of short time scale events from a product analysis. Such an experiment depends critically upon the trapping reaction matching in detail the proposed kinetic model, without the participation of other fast reactions depleting the initial radical population. Many of the previous studies were condition-limited by the necessity of having adequate ESR signals simultaneously from two radical populations, produced before and after the ticking of the radical clock. Finally, few kinetic studies have been performed in aqueous solution, the ubiquitous solvent of biological systems,[18-22] and these did not directly observe the kinetics of the spin adduct. Since several studies indicated conflict with direct kinetic analysis by pulse radiolysis techniques[13,14] and differential trapping efficiencies have been proposed for organosulfur and pyrimidine radicals,[23,24] we have initiated direct measurements of spin trapping kinetics by using time-resolved electron spin resonance techniques (TRESR).

Pulse radiolysis methods can be used in combination with TRESR to record the production and evolution of a free-radical population on a microsecond time scale, allowing one to correlate the measured decay of a transient radical with the growth of the spin adduct radical. Pulse radiolysis produces 40 micromolar initial radical populations within 0.5 μs, to give high detection efficiency, while the use of a fast flow system guarantees that secondary products of free-radical reactions can not build up to cause unseen kinetic complications. Finally, direct measurement of radical kinetics allows verification of the correctness of the kinetic model used to fit the overall trapping process.

Previous work in these laboratories has demonstrated the utility of the nitromethane *aci*-anion as a spin trap for a variety of organic and inorganic radicals;[25-27] for a recent review, see ref 28. A number of adducts have been characterized, and the specific variation of the hyperfine parameters with the nature of the radical which has been added is such that a large number of adducts can be distinguished and overlap of the ESR lines of two adducts is minimized. An additional advantage is provided by the relatively narrow lines and, in many cases, the absence of unresolved splittings. These spin adducts are not persistent, and so nitromethane does not fully qualify as a spin trap in the narrowest sense. However, the adducts have lifetimes which are longer enough than those of the initial radicals that this system has proved to be very useful where continuous production of radicals is possible. In this work, we have directly measured the formation rates of the adducts produced when various radicals react with the *aci*-anion of nitromethane in alkaline aqueous solution. In a number of cases, the corresponding decay of the parent radical has also been followed and found to be complementary with the formation of the adduct. Further measurements on other more conventional spin traps are planned now that experience has been gained in the present work.

Table I. ESR Parameters for Nitromethane Radical Adducts[a]

radical (parent)	*g* factor	a^{N} [b] (G)	a^{H} [c] (G)	addtnl resolved couplings (G)	
$CH_3NO_2^-$ (e^-_{aq})	2.00497	26.04	12.15 (3)		
$CH_2NO_2^-$ OH (OH)	2.00492	24.66	8.60 (2)		
$CH_2NO_2^-$ $C(OH)H_2$ ($C(OH)H_2$)	2.00498	25.48	10.67 (2)	$a^{H}_{H_\gamma}$	0.45 (2)
$CH_2NO_2^-$ $C(CH_3)_2OH$ ($C(CH_3)_2OH$)	2.00495	24.40	10.06 (2)		
$CH_2NO_2^-$ CO_2 (CO_2^-)	2.00491	24.55	8.51 (2)		
$CH_2NO_2^-$ SO_3 (SO_3^-)	2.00498	22.19	7.50 (2)		
$CH_2NO_2^-$ CH_2-CO_2^- ($CH_2CO_2^-$)	2.00501	26.00	10.0 (2)	$a^{H}_{H_\gamma}$	0.70 (2)
$CH_2NO_2^-$ C_6H_4-CO_2 ((C_6H_4)-CO_2^-)	2.00497	25.87	9.82 (2)		
CH_2-NO_2^- CH_3 (CH_3)	2.00497	26.04	9.68 (2)	$a^{H}_{H_\gamma}$	0.45 (3)
CH_2-NO_2^- $C(O)NH_2$ ($C(O)NH_2$)	2.00503	25.32	8.03 (2)	$a^{N}_{NH_2}$ $a^{H}_{NH_2}$	0.49 0.37

[a] All parameters are measured from steady-state ESR spectra at 12 °C and are corrected for second-order shifts.[38] *g* factors are ±0.00002; hyperfine couplings are ±0.01 G. [b] Coupling to nitrogen of nitro group. [c] Coupling to β methylene protons.

Experimental Section

All solutions were prepared in reagent grade water from a Millipore Milli-Q water system. Solutions were 0.5–5 mM in nitromethane (Aldrich) and unless otherwise noted were adjusted to pH 11.3 with KOH (Fisher or Baker). Substrates for radical production were as follows: methanol (0.25 M, Aldrich gold label), isopropyl alcohol (0.25 M, Fisher ACS or Baker), sodium acetate (0.5 M, Fisher or Baker), sodium sulfite (0.05 M, MCB), sodium formate (0.1 M, Fisher), dimethyl sulfoxide (0.1 M, Burdick and Jackson), *p*-bromobenzoic acid (1 mM, Aldrich), and formamide (0.1 M, Eastman or Fisher). Hydroxyl radical oxidation was used to produce all the parent radicals for this study, with the exception of the *p*-carboxyphenyl radical, which was produced by dissociative electron attachment to *p*-bromobenzoic acid. In the latter case, ultrahigh purity nitrogen (Mittler) was used to deoxygenate the solution; otherwise, nitrous oxide (Mittler U.S.P.) was used to convert solvated electrons to hydroxyl radicals.

(5) Fessenden, R. W.; Schuler, R. H. In *Advances in Radiation Chemistry*; Burton, M., Magee, J. C., Eds.; Interscience: New York, 1970; Vol. 2, pp 1–176.
(6) Griller, D.; Ingold, K. U. *Acc. Chem. Res.* **1980**, *13*, 317–23.
(7) Janzen, E. G.; Evans, C. A. *J. Am. Chem. Soc.* **1973**, *95*, 8205–6.
(8) Haire, D. L.; Janzen, E. G. *Can. J. Chem.* **1982**, *60*, 1514–22.
(9) Ledwith, A.; Russell, P. J.; Sutcliffe, L. H. *Proc. R. Soc. London A* **1973**, *332*, 151–66.
(10) Sargent, F. P. *J. Phys. Chem.* **1977**, *81*, 89–90.
(11) Perkins, M. J.; Roberts, B. P. *J. Chem. Soc., Perkin Trans. 2* **1974**, 297–304.
(12) Perkins, M. J.; Roberts, B. P. *J. Chem. Soc., Perkin Trans. 2* **1975**, 77–84.
(13) Janzen, E. G.; Evans, C. A. *J. Am. Chem. Soc.* **1975**, *97*, 205–6.
(14) Janzen, E. G.; Nutter, D. E., Jr.; Evans, C. A. *J. Phys. Chem.* **1975**, *79*, 1983–4.
(15) Lilie, J.; Behar, D.; Sujdak, R. J.; Schuler, R. H. *J. Phys. Chem.* **1972**, *76*, 2517.
(16) Schmid, P.; Ingold, K. U. *J. Am. Chem. Soc.* **1978**, *100*, 2493.
(17) Maeda, Y.; Ingold, K. U. *J. Am. Chem. Soc.* **1979**, *101*, 4975–81.
(18) Castelhano, A. L.; Perkins, M. J.; Griller, D. *Can. J. Chem.* **1983**, *61*, 298–9.
(19) Neta, P.; Steenken, S.; Janzen, E. G.; Shetty, R. V. *J. Phys. Chem.* **1980**, *84*, 532–34.
(20) Sridhar, R.; Beaumont, P. C.; Powers, E. L. *J. Radioanal. Nuc. Chem.* **1986**, *101*, 227–37.
(21) Greenstock, C. L.; Wiebe, R. H. *Can. J. Chem.* **1982**, *60*, 1560–4.
(22) Marriott, P. R.; Perkins, M. J.; Griller, D. *Can. J. Chem.* **1980**, *58*, 803–7.
(23) Spalletta, R. A.; Bernhard, W. A. *Radiat. Res.* **1982**, *89*, 11–24.
(24) Taniguchi, H. *J. Phys. Chem.* **1984**, *88*, 6245–50.
(25) Eiben, K.; Fessenden, R. W. *J. Phys. Chem.* **1971**, *75*, 1186–201.
(26) Eiben, K.; Fessenden, R. W. *J. Phys. Chem.* **1968**, *72*, 3387–93.
(27) Laroff, G. P.; Fessenden, R. W. *J. Magn. Reson.* **1973**, *9*, 434–7.
(28) Gilbert, B. C.; Norman, R. O. C. *Can. J. Chem.* **1982**, *60*, 1379–91.

ESR[25,29] spectra of steady-state concentrations of nitromethane spin adducts or parent radicals in flowing aqueous solutions were observed during continuous irradiation with a 2.5-μA beam of 2.8-MeV electrons. These spectra were recorded at 9.2 GHz in second derivative presentation by simultaneous field modulation and phase sensitive detection at 100 kHz and 200 Hz by using an ESR spectrometer constructed from Varian Century Series Mark III components. Magnetic field measurements were by NMR methods,[29] with g factors measured with respect to that of the sulfite radical anion, $g = 2.00307$.[30] Real-time data digitization and magnetic field–microwave frequency locking were accomplished by using a dedicated DEC LSI-11 microcomputer.

TRESR kinetic data curves were recorded with the spectrometer described above during irradiation with a 2.8 MeV, 50 milliampere pulsed electron beam of 0.5 μs duration and 103 Hz repetition rate. Initial radical concentrations were estimated to be 40 micromolar by measurement of the second-order decay of the sulfite radical anion produced under identical conditions. Data were recorded at the field positions determined in the steady-state experiment, avoiding any overlapping absorptions. The direct detection TRESR signal channel was as described previously,[31] with field stepping base line correction employed on alternant beam pulses. Typical kinetic curves were linear averages of 8000 experiments.

The solutions used for all experiments were cooled before irradiation to prevent bubbling within the microwave cavity. The temperature of the irradiated solution was ~12 °C. The flow rate for SSESR experiments was 20 mL/min. The rate for time-resolved studies was 110 mL/min to ensure complete removal of long-lived spin adducts between electron beam pulses.

Results and Discussion

Hyperfine couplings and g factors for the nitromethane spin adducts were measured with steady-state ESR techniques and are listed in Table I. Line positions for the parent radicals were also established in this way. In all cases, the ESR parameters agreed with published values. Two parent species could not readily be observed. The methyl radical has broad lines as a result of fast spin rotation relaxation, while the broad absorption from the formate radical, $^{\bullet}CO_2^-$, is hidden under the intense signal from the quartz ESR cell. All other parent radicals had narrow lines which are sufficiently separated from those of the spin adduct that TRESR kinetic studies could be carried out on both species. The adduct radicals were usually followed by using one (or more) of the lines associated with the low field ^{14}N spin state.

Typical SSESR spectra of various adducts are shown in Figures 1 and 2. Irradiation of aqueous alkaline solutions containing 5 mM nitromethane (NM) at pH 11.3 results in the ESR spectrum of Figure 1a. This pH was chosen so that the nitromethane was 90% in the *aci*-anion form ($CH_2{=}NO_2^-$), the active form for spin trapping. Pulse radiolysis studies[32,33] show that the solvated electron and hydroxyl radical produced in the radiolysis of water react quickly with NM *aci*-anion (6.6×10^9 and 8.5×10^9 M^{-1} s^{-1}, respectively). Figure 1a shows ESR lines from the NM electron adduct (the anion radical, $CH_3NO_2^-$) and the NM hydroxyl radical adduct ($HOCH_2NO_2^-$). Spectra obtained upon irradiation of solutions of NM which also contain methanol (Figure 1b), isopropyl alcohol (Figure 1c), and formate (Figure 2) are also shown. The main lines seen with the two alcohols are, in each case, from the NM anion radical and the corresponding adducts. The radical formed by trapping $^{\bullet}CH_2OH$ shows small splittings from the CH_2 protons which are in the γ position in the adduct. Only the adduct is seen in the case of formate (Figure 2). In this instance, it is possible to see lines from radicals containing ^{13}C at the β and γ positions. The hyperfine couplings are 1.45 G for the β carbon (this work), and 10.75 G for the γ carbon.[27] The individual spectra show hyperfine couplings to the nitrogen of the nitro moiety and the adjacent methylenic protons, features common to all NM adducts. The width of the lines where no further splittings are possible, as with the anion, is controlled by the nitrogen hyperfine and g factor anisotropy. The resultant line widths are about 0.25 G. This width indicates a relaxation time of roughly 0.25 μs for NM adduct radicals. A list of the hyperfine parameters of the adducts observed here is given in Table I.

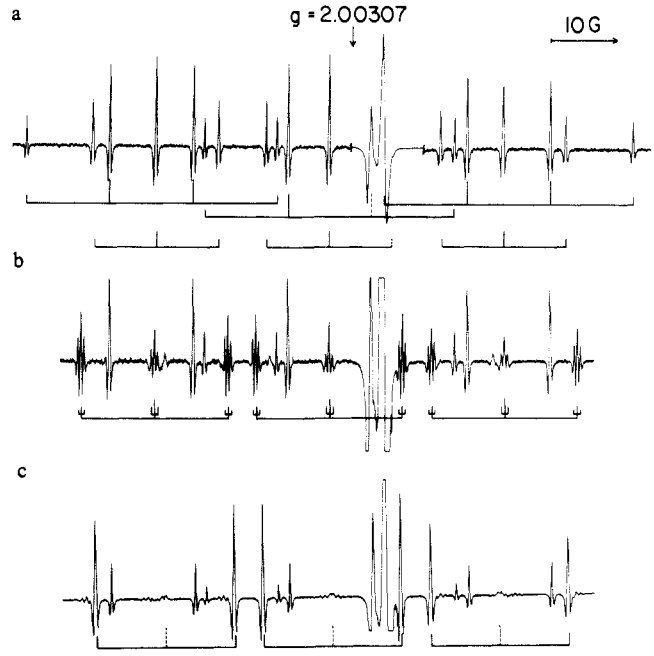

Figure 1. Second derivative steady-state ESR spectra observed with nitromethane itself (a), nitromethane and methanol (b), and nitromethane and isopropyl alcohol (c) at pH 11.3. All spectra are presented with magnetic field increasing from left to right. Solution temperature was ~12 °C. Stick spectra below the experimental spectra mark the lines of the main radicals. The large double-peaked line to the right of the center is from the silica cell. At the top are shown the lines of the nitromethane anion radical (three quartets) and those of the OH adduct (three triplets). In the center, the lines of the CH_2OH adduct ($HOCH_2CH_2NO_2^-$) are marked and at the bottom those of the adduct of $(CH_3)_2COH$. All spectra show hyperfine couplings to the nitro nitrogen and β methylenic protons. The spectrum at the center shows small splittings by the β CH_2 protons. At the bottom, the central lines of the triplets are broadened by hindered rotation. The spectra from both alcohol solutions also show lines from the NM anion radical.

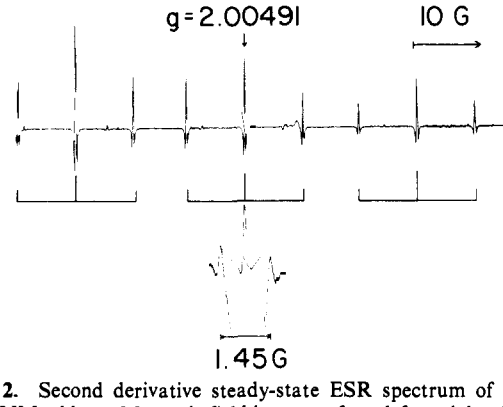

Figure 2. Second derivative steady-state ESR spectrum of formate radical NM adduct. Magnetic field increases from left to right. Solution temperature was ~12 °C. Stick spectra show hyperfine couplings to nitro nitrogen and β methylenic protons. Inset shows satellite doublet (gain ×100) centered about central line of the main spectrum, with peak intensity 0.5% that of the main line. Splitting of 1.45 G is due to natural abundance carbon-13 adjacent to the nitro function of the adduct.

The spectral intensity of a radical in a continuous irradiation experiment is determined by both its production and disappearance rates.[5] Casual examination of Figure 1 (parts b and c) reveals large NM anion radical signals, while Figure 2 shows no apparent NM anion radical. The large NM anion radical signal in the first two cases could be explained in two ways. Firstly, there could be small amounts of NM anion radicals formed that have a much

(29) Fessenden, R. W.; Schuler, R. H. *J. Chem. Phys.* **1963**, *39*, 2147–95.
(30) Chawla, O. P.; Arthur, N. L.; Fessenden, R. W. *J. Phys. Chem.* **1973**, *77*, 772–6.
(31) Verma, N. C.; Fessenden, R. W. *J. Chem. Phys.* **1976**, *65*, 2139–55.
(32) Asmus, K.-D.; Taub, I. A. *J. Phys. Chem.* **1968**, *72*, 3382–7.
(33) Asmus, K.-D.; Henglein, A.; Beck, G. *Ber. Bunsenges. Phys. Chem.* **1966**, *70*, 459–66.

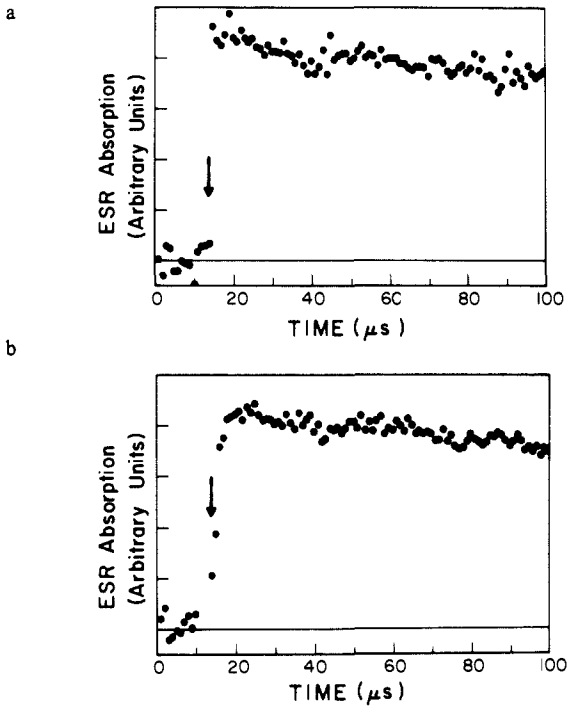

Figure 3. (a) TRESR kinetic profile of hydroxyl radical NM adduct. (b) TRESR kinetic profile of solvated electron NM adduct. Nitromethane concentration is 5 mM at pH 11.3. The solution is deoxygenated with nitrogen gas. The 0.5 μs electron beam pulse occurs at the time indicated by the vertical arrow.

longer lifetime than the alcohol radical NM adducts. The large NM anion signal therefore would mislead one into thinking the relative amounts of NM adduct species were comparable. Secondly, large amounts of NM anion radical could be formed initially, with a lifetime comparable to or shorter than that of the alcohol radical adduct. These two cases cannot be easily differentiated from steady-state ESR data. On the other hand, the absence of a multiple spectrum, as in the case of the formate radical NM adduct ESR spectrum does not guarantee that the trapping reaction is fast (vide infra) or free from complications. TRESR, however, allows unambiguous determination of trapping efficiency and kinetics.

Various parent radicals for the time-resolved experiments were formed by reaction of OH or e_{aq}^- with a substrate. The concentrations were chosen so that the amount of NM to be added did not compete for the primary radical. In some cases (such as acetate) some reduction in the yield of the desired parent radical occurred at the highest NM concentrations. Formation of the parent radicals was complete in much less than 1 μs.

Kinetic traces for the NM anion radical and the NM hydroxyl radical adduct are shown in Figure 3. The rapid rise of the ESR kinetic traces verifies the conclusions reached above regarding the spin relaxation times. Under these conditions, the curve of ESR absorption versus time reflects the chemical kinetics of the radical and is not significantly affected by any transient affects on the spin system which would make the ESR signal not follow the radical concentration. Thus the ESR kinetic curves are expected to follow simple exponential growth reflecting pseudo-first-order kinetics. The situation for the disappearance of a given parent radical will depend on its particular spin relaxation time. However, all of the radicals to be studied have relaxation times no longer than about 1.5 μs. In addition, the chemical decay will add to the natural relaxation time to shorten the effective relaxation time as the decay rate is made faster by higher NM concentrations.[34] In practice, it was found that the ESR signals during the decay of the parent radicals could usually be fit to simple exponential curves at the microwave power levels used. In some instances, as in the case of $^{\bullet}CH_2CO_2^-$ (see below), it was necessary to ignore the first part of the decay and analyze the decay after an initial transient of the spin system had decayed.

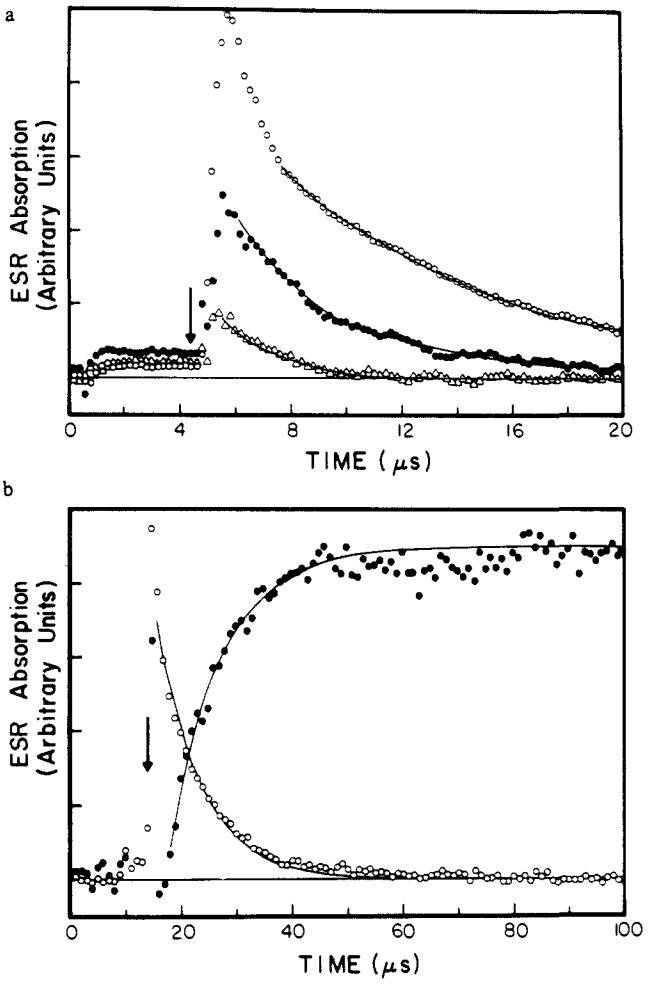

Figure 4. (a) TRESR kinetic profile of acetate radical decay in a N_2O saturated aqueous solution of 0.5 M acetate, pH 11.4, containing 1 (○), 2.5 (●), and 5 mM (△) nitromethane. (b) TRESR kinetic profile of acetate radical signal decay and concomitant growth of the adduct in 1 mM soluton. The 0.5 μs electron beam pulse occurs at the time indicated by the vertical arrow. The initial fast decay of the curve for 1 mM nitromethane at the top is a transient effect of the spin system (Torrey oscillation). The decay after about 8 μs can be analyzed by simple kinetics.

The radicals trapped in this study can be grouped into three categories. We will consider them separately below. The trapping rate constants for all systems studied are shown in Table II.

Alkyl Radicals (Nonreducing). The prototype radical of this group is the methyl radical. However, since the width of its lines prevents detection with high sensitivity, it was not possible to study both the parent radical decay and the adduct formation. The acetate radical, $^{\bullet}CH_2CO_2^-$, was chosen as the representative of this group and studied in detail. TRESR kinetic traces are shown in Figure 4a for the decay of acetate radical in the presence of 1, 2.5, and 5 mM NM at pH 11.4. As the concentration of NM is increased, the decay becomes faster. These curves were analyzed as first-order decays. A plot of pseudo-first-order rate constant against concentration of NM was used to determine the second-order rate constant. Figure 4b shows the acetate radical decay and the corresponding growth of the adduct at 1 mM NM. The half lives for the two curves shown are in agreement at 5.3 and 6.7 μs, respectively. In Figure 4a it is also seen that the initial amplitude of the ESR signal for the parent radical is reduced as the reaction becomes faster. This effect is caused by competition between acetate and NM for OH and also by the increase in effective spin relaxation time as the chemical decay rate becomes comparable to the spin relaxation.[34] The rate constant for trapping

(34) Fessenden, R. W. *J. Chem. Phys.* **1973**, *58*, 2489–500.

Table II. Second-Order Rate Constants for Nitromethane Radical Trapping Reactions (M^{-1} s^{-1})[e]

parent radical	parent decay	NM adduct growth	NM anion growth
$SO_3^{\bullet-}$	1.0×10^8	1.2×10^8	*b*
$CH_2CO_2^-$	8.8×10^7	7.9×10^7	*b*
CH_3	*a*	1.0×10^8	*b*
CH_2O^-	2.6×10^7	2.1×10^7	2.1×10^7
$C(CH_3)_2O^-$ (pH 13.0)	4.0×10^7	3.4×10^7	*b*
$C(CH_3)_2OH$ (pH 9.15)	1.2×10^7	*c*	$\sim 1.2 \times 10^7$
$C(CH_3)_2OH$	5.0×10^7	5.0×10^7	*b*
$CO_2^{\bullet-}$	*d*	1.4×10^7	*b*
p-CO_2^--phenyl	3.6×10^8	3.8×10^8	*b*
C(O)-NH_2	2.4×10^8		*b*

[a] Line broadening due to spin rotation relaxation precludes measurement. [b] No anion radical absorption observed. [c] No absorption of adduct observed at short time after beam pulse. [d] Line broadening precludes TRESR measurement. [e] pH 11.3 unless otherwise noted.

in this case is 8×10^7 M^{-1} s^{-1}. The rate constants for trapping are summarized in Table II.

Methyl radical was studied through the formation kinetics of the adduct. It was formed by the reaction of OH with dimethyl sulfoxide.[35] A similar rate constant of 1×10^8 was found for the growth of the CH_3 adduct to NM. The absence of charge on this radical (relative to $CH_2CO_2^-$) only increased the rate constant a small amount. For neither of these radicals was any significant formation of the NM electron adduct detected.

σ Radicals. Carbon-centered σ radicals are generally more reactive than alkyl π radicals, and so it was of interest to see if their reactivity extends to the addition of NM. Two radicals of this type were investigated: 4-carboxyphenyl radical produced by the reaction of e_{aq}^- with 4-bromobenzoate and $CONH_2$ formed by the reaction of OH with formamide. The trapping rate constants are 3.7×10^8 and 2.4×10^8 M^{-1} s^{-1}, respectively. These values are, indeed, somewhat larger than those of the alkyl radicals in the previous group. Neither of the σ radicals showed a tendency to reduce NM to the electron adduct.

It is appropriate to include both $^{\bullet}SO_3^-$ and $^{\bullet}CO_2^-$ in this group since they are both σ radicals and both form adducts with NM. The rate constants found for $^{\bullet}SO_3^-$ decay and adduct formation agree at 1×10^8 M^{-1} s^{-1}. This value is less than those for the two carbon-centered σ radicals and is similar to values for the alkyl radicals. The rate constant for CO_2^- is an order of magnitude less at 1.4×10^7 M^{-1} s^{-1} so this radical seems to be in a special class by itself.

Hydroxyalkyl Radicals. The radicals in this group include the hydroxyalkyl radicals $^{\bullet}CH_2OH$ and $(CH_3)_2C^{\bullet}OH$. The state of ionization of the alcohol radical provides another variable to these experiments. The pK of the methanol radical is 10.7, so the predominant form is $^{\bullet}CH_2O^-$. Although the steady-state ESR spectrum shows appreciable intensity from the expected adduct, TRESR shows no significant formation of this species immediately after the elecron beam pulse. The NM methanol radical adduct and NM electron adduct grow slowly with concomitant decay of the methanol radical absorption. In this case the reduction of the NM trap competes favorably with adduct formation. Three quarters of the methanol radicals form NM methanol radical adduct, accounting for the signal seen in the steady-state experiments. The remaining 25% of the methanol radicals reduce NM to the NM anion radical.

The situation with the isopropyl alcohol radical, $(CH_3)_2COH$ ($pK_a = 12.03$[36]), is more complicated in that it is not predominantly in one form at the pH normally used in these experiments. To determine the behavior more thoroughly, experiments were carried out at several pH values. At pH 9.15 in borate buffer the isopropyl alcohol radical and NM are neutral species; reaction by electron transfer leads to the electron adduct. At pH 11.3, NM is 90% dissociated to the active *aci*-anion form, while isopropyl alcohol radicals are 84% protonated. Here the isopropyl alcohol radical adduct is the main product on the time scale of the pulse experiments, and little anion is found. The trapping rate at pH 11.3 is ~2.5 higher than the electron-transfer rate at pH 9.15. At pH 13.0, both NM and isopropyl alcohol radical are predominantly in their dissociated forms. The only product observed is the adduct of the isopropyl alcohol radical, but the trapping rate has diminished to 0.68 at pH 11.3. The negative charge on the two reactants probably causes the reduction in rate constant. These examples indicate that, with NM, electron transfer may compete successfully with radical trapping.

Table III. Previously Determined Trapping Rate Constants (M^{-1} s^{-1})

spin trap[a]	parent radical	solvent	rate	ref
PBN	benzoyloxy	benzene	10^5–10^6	4
PBN	*tert*-butoxy	benzene	6.8×10^5	7
PBN	*tert*-butoxy	benzene	5.5×10^6	7
MNP	*tert*-butoxy	benzene	1.5×10^6	7
MNP	*tert*-butoxycarbonyl	di-*tert*-butyl peroxide	1.1×10^6	11
MNP	methoxy	methanol	$>6 \times 10^7$	9
PBN	phenyl	benzene	1.2×10^7	13
PBN	benzoyloxy	benzene	4×10^7	13
MNP	di-*tert*-butyoxymethyl	benzene	$\sim 10^6$	12
MNP	methoxy	methanol	1.3×10^8	10
MNP	*n*-hexyl	benzene	8.8×10^6	37
		methanol	1.16×10^7	
		acetonitrile	1.31×10^7	
PBN	*n*-hexyl	benzene	1.3×10^5	37
		methanol	1.2×10^6	
		acetonitrile	1.6×10^6	
MNP	6-hepten-2-yl	benzene	6.1×10^6	17
PBN	6-hepten-2-yl	benzene	0.68×10^5	17

[a] MNP = 2-methyl-2-nitroso-propane; PBN = *N*-(*tert*-butyl)-*a*-phenylnitrone.

Further Discussion

The quantitative data presented above spans a 30-fold variation in trapping rate constants. Such a variation is surprising for simple carbon-centered radicals. The main variation (toward lower rate constant) is for the reducing radicals such as $^{\bullet}C(CH_3)_2O^-$, $^{\bullet}CH_2O^-$, and $^{\bullet}CO_2^-$. These radicals are less electrophilic than their alkyl radical counterparts and so less readily take part in addition reactions.

Previous determinations of trapping rates[8-12,16-22,37] (with one exception, see below) are not directly comparable with our results, as other spin traps as well as nonaqueous solvents were used. A sampling of these results for the popular spin traps PBN (*n*-(*tert*-butyl)-α-phenylnitrone) and MNP (2-methyl-2-nitroso-propane) is reproduced in Table III. The trapping rate constant for primary alkyl radicals in our work is $\sim 10^8$ M^{-1} s^{-1}. In previous studies, only methoxy radical trapping by MNP in methanol[9,10] and *tert*-butoxyl radical trapping by DMPO in benzene[7] compares with this rate. Ingold and co-workers[37] have shown that in solvents of increasing dielectric constants, trapping rates for a given nitrone spin trap will increase. The effect is attributed to the stabilization of the strong nitrogen–oxygen dipole forming in the transition state leading to the nitroxide. The NM *aci*-anion is charged before trapping occurs and is stabilized by the solvating water molecules. The NM adduct radical electronic structure is very much like that of the trap, so that trapping rate is maximized for NM in the aqueous system. As an alkyl radical trap, aqueous NM is at least an order of magnitude faster than nitroso or nitrone traps in moderately polar solvents.

To our knowledge, only Maeda and Ingold[17] have studied trapping of secondary alkyl radicals, finding that 6-hepten-2-yl radicals were trapped by MNP more slowly than its primary analogue, *n*-hexyl radical (6.1×10^6 versus 8.8×10^6 M^{-1} s^{-1}) in benzene solution. The rates using PBN as the trap were 0.68×10^5 versus 1.3×10^5 M^{-1} s^{-1}. This trend is also observed in the aqueous NM system, where isopropyl alcohol radical is trapped

(35) Lagercrantz, C.; Forshult, S. *Acta Chem. Scand.* **1969**, *23*, 811–7.
(36) Laroff, G. P.; Fessenden, R. W. *J. Phys. Chem.* **1973**, *77*, 1283–8.
(37) Maeda, Y.; Schmid, P.; Griller, D.; Ingold, K. U. *J. Chem. Soc., Chem. Commun.* **1978**, 525–6.
(38) Fessenden, R. W. *J. Chem. Phys.* **1962**, *37*, 747–50.

with half the rate of methyl radical trapping (5.0×10^7 versus 1×10^8 M^{-1} s^{-1}).

σ radical trapping is relatively unexplored in the literature. A single value of 5×10^8 M^{-1} s^{-1} hs been reported for the trapping of CF_3 by NM.[15] This value is rather similar to those for 4-carboxyphenyl and $CONH_2$ found here. The value for $^{\bullet}CO_2^-$ clearly shows this radical to be different than the other σ radicals. We note the formamide radical, $^{\bullet}CONH_2$, is a good model for a fragmented peptide bond in biological systems. In biological systems, where spin trapping has been utilized to its greatest extent, both σ and π radicals are produced, in environments of greatly varying polarity and effective pH. Reliable quantitative (and in some cases qualitative) data on biological free-radical reactions will not be available until the observed variability of free radical trapping rates can be understood and measured. We believe the TRESR pulse radiolysis method is uniquely suited to test the efficiency and selectivity of spin trapping reactions.

Acknowledgment. We gratefully acknowledge helpful conversations with Professors David Armstrong and William Bernhard. We thank Ian Duncanson of the NDRL glass shop for design assistance and construction of free flow ESR flat cells.

The r_α Structures of Pyrazine and Pyrimidine by the Combined Analysis of Electron Diffraction, Liquid-Crystal NMR, and Rotational Data

Stephen Cradock, Phillip B. Liescheski, David W. H. Rankin,* and Heather E. Robertson

Contribution from the Department of Chemistry, University of Edinburgh, West Mains Road, Edinburgh EH9 3JJ, Scotland, United Kingdom. *Received September 10, 1987*

Abstract: The molecular structures of pyrazine and pyrimidine have been determined by combined analyses of data obtained by gas-phase electron diffraction, rotational spectroscopy, and liquid-crystal NMR. The studies illustrate the complementary nature of information obtained by liquid-crystal NMR spectroscopy and that obtained by electron diffraction and rotational spectroscopy. Geometrical parameters (r_α) for pyrazine from the combined analysis are as follows: rCH = 108.31 (37), rCN = 133.76 (13), rCC = 139.68 (30) pm; $\angle$CNC = 115.65 (24), $\angle$CCH = 119.96 (8)°. Geometrical parameters (r_α) for pyrimidine from the combined analysis are the following: rC(5)H(9) = 108.7 (3), rC(4)H(8) = 107.9 (2), rC(2)H(7) = 108.2 (4), rCC = 139.3 (3), rC(4)N = 135.0 (7), rC(2)N = 132.8 (7) pm; $\angle$CCC = 117.8 (2), $\angle$C(5)C(4)H(8) = 120.9 (3), $\angle$CCN = 121.2 (3)°.

The chemical properties of a compound are known to be dependent upon its structure, so the knowledge of accurate structures and methods to obtain them are essential to chemistry. For many years, the structures of gas-phase molecules were determined either by electron diffraction (ED) or rotational spectroscopy. In ED, the molecules under investigation are allowed to scatter an electron beam. From the interference pattern of the scattered electrons, distances between atoms can be determined, and so information on the three-dimensional structure of the molecule can be deduced. In rotational spectroscopy, the moments of inertia of the molecule are obtained from its measured rotation constants and used to obtain structural information. Since 1962, the NMR spectra of partially oriented molecules have been used to obtain molecular structure in the liquid phase.[1] In liquid-crystal NMR (LCNMR) spectroscopy, the liquid-crystal solvent molecules in the presence of the magnetic field of the NMR spectrometer partially orientate the solute molecules under investigation. In this anisotropic fluid the intramolecular direct dipolar couplings between spin $^1/_2$ nuclei in the solute molecule no longer average to 0, and so become measurable. The direct dipolar couplings are spacially dependent internuclear interactions, so one can extract structural information from them.

Unfortunately, all of these techniques have their limitations. In rotational spectroscopy, three rotation constants at most can be measured for any single isotopic species of a particular compound. For all but the simplest compounds several isotopically substituted species must be prepared and studied in order to obtain enough structural information. To complicate the situation further, some elements, such as fluorine and phosphorus, have only one natural (stable) isotope, which can lead to a practical restriction on the number of possible isotopic species. Finally, a dipole moment is required on the molecule in order to observe its microwave spectrum. In electron diffraction, three-dimensional information (molecular structure) is reduced to one-dimensional data (radial distribution curve) since the electrons are scattered by an ensemble of randomly oriented molecules. As a result of this reduction, data on different interatomic distances that are similar in length are correlated, and thus poorly determined. Also, positions of light atoms, particularly hydrogen, are not well determined in the presence of heavy atoms, owing to their lower electron-scattering ability. In LCNMR, useful information can only be had from spin $^1/_2$ nuclei. Also, it is difficult to separate the direct dipolar couplings from their corresponding anisotropic indirect couplings, which become significant for nuclei larger than the proton. As a result, one tends to be restricted to couplings which involve protons. Finally, the orientation parameters, which are additional unknowns in the analysis of LCNMR data, are correlated to information on the absolute size of the molecule, so only bond angles and ratios of interatomic distances can be determined.

The information given by ED tends to be complementary to that given by LCNMR. It has been shown that combining the data from the two techniques can be useful.[2,3] There are three major benefits in performing a joint analysis. Firstly, ED data easily give information on the absolute size of a molecule, which is absent in LCNMR data. Secondly, the ratio of interatomic distances of similar length can be obtained from the dipolar couplings and used to reduce the correlation found using ED alone.

(1) Englert, G.; Saupe, A. *Z. Naturforsch., A* **1962**, *19*, 172-177. Saupe, A.; Englert, G. *Phys. Rev. Lett.* **1963**, *11*, 462-464.

(2) Boyd, A. S. F.; Laurenson, G. S.; Rankin, D. W. H. *J. Mol. Struct.* **1981**, *71*, 217-226.

(3) Blair, P. D.; Cradock, S.; Rankin, D. W. H. *J. Chem. Soc., Dalton Trans.* **1985**, 755-759.

0002-7863/88/1510-2758$01.50/0